JBC Papers in Press. Published on April 13, 2015 as Manuscript M114.606608
The latest version is at http://www.jbc.org/cgi/doi/10.1074/jbc.M114.606608

Metabotropic glutamate receptors: modulators of context-dependent feeding behaviour in *C. elegans*.

James Dillon[1], Christopher J. Franks[1], Caitriona Murray[2], Richard J. Edwards[3], Fernando Calahorro[1], Takeshi Ishihara[4], Isao Katsura[5], Lindy Holden-Dye[1] and Vincent O'Connor[1]

[1] Centre for Biological Sciences, University of Southampton, University Road, Southampton, SO17 1BJ
[2]Ramaciotti Centre for Genomics, The University of New South Wales, Kensington, NSW 2052, Australia
[3]School of Biotechnology and Biomolecular Sciences, The University of New South Wales, Kensington, NSW 2052, Australia
[4]Department of Biology, Graduate School of Science, Kyushu University, 6-10-1, Hakozaki, Higashi-ku, Fukuoka 812-8581, Japan
[5]National Institute of Genetics, Yata 1111, Mishima, Shizuoka-ken, 411-8540, Japan

*Running Title: mGluRs in *C. elegans*

To whom correspondence should be addressed: James Dillon/Vincent O'Connor. Centre for Biological Sciences, University of Southampton, University Road, Southampton SO17 1BJ, Hants, UK. E.mail: jcd@soton.ac.uk/voconno@soton.ac.uk

Key words: metabotropic glutamate receptors (mGluR); optogenetics; *Caenorhabditis elegans* (*C. elegans*); electrophysiology; invertebrate

Background: *C. elegans* expresses three metabotropic glutamate receptors: *mgl-1*, *mgl-2* and *mgl-3*.
Results: *mgl-1* and *mgl-3*, but not *mgl-2*, modulate activity in the neural circuit underlying feeding behaviour.
Conclusion: *mgl-1* is the major contributor to the inhibitory tone of the feeding circuit and context-dependent feeding behaviour.
Significance: *C. elegans* provides a model for systems level understanding of metabotropic glutamate receptors.

ABSTRACT

Glutamatergic neurotransmission is evolutionarily conserved across animal phyla. A major class of glutamate receptors are the metabotropic glutamate receptors (mGluRs). In *C. elegans* three mGluR genes *mgl-1*, *mgl-2* and *mgl-3* are organised into three sub-groups, similar to their mammalian counterparts. Cellular reporters identified expression of the *mgl*s in the nervous system of *C. elegans* and overlapping expression in the pharyngeal microcircuit that controls pharyngeal muscle activity and feeding behaviour. The overlapping expression of *mgl*s within this circuit allowed investigation of receptor signalling per se and in the context of receptor interactions within a neural network that regulates feeding. We utilized the pharmacological manipulation of neuronally regulated pumping of the pharyngeal muscle in wild type and mutants to investigate *mgl* function. This defined a net *mgl-1* dependent inhibition of pharyngeal pumping which is modulated by *mgl-3* excitation. Optogenetic activation of the pharyngeal glutamatergic inputs combined with electrophysiological recordings from the isolated pharyngeal preparations provided further evidence for a presynaptic *mgl-1* dependent regulation of pharyngeal activity. Analysis of *mgl-1*, *mgl-2* and *mgl-3* mutant feeding behaviour in the intact organism after acute food removal identified a significant role for *mgl-1*in the regulation of an adaptive feeding response. Our data describes the molecular and cellular organisation of *mgl-1*, *mgl-2* and *mgl-3*. Pharmacological analysis identified that in these paradigms *mgl-1* and *mgl-3*, but not *mgl-2*, can modulate the pharyngeal microcircuit. Behavioural analysis identified *mgl-1* as a significant determinant of the glutamate-dependent modulation of feeding, further highlighting the significance of mGluRs in complex *C. elegans* behaviour.

INTRODUCTION

In mammals glutamate signals broadly via two classes of receptor, these are the

ionotropic (iGluR) and metabotropic (mGluR) glutamate receptors (1,2). Metabotropic glutamate receptors (mGluRs) are G-protein coupled receptors and perform an important neuromodulatory role in glutamatergic transmission within the mammalian nervous system (3,4). The importance of this class of receptor is highlighted by their involvement in a number of different neurological conditions, including anxiety, autism and schizophrenia (5,6). Interestingly, it has been proposed that each of these conditions involves a loss of the balance between cellular inhibition and excitation within the context of discrete microcircuits (7-9). As neuromodulators mGluRs represent attractive targets to manipulate the excitatory-inhibitory balance and alleviate the behavioural dysfunction and sensory deficits associated with these conditions (6,10). Hence, understanding of mGluR contribution to the balance of activity within a microcircuit is potentially beneficial within the broader context of neurological disorders where this imbalance has been suggested as an underlying cause.

Both iGluR and mGluR classes of receptor are conserved within the genome of the model organism *C. elegans*. In *C. elegans* the iGluR subfamily is well characterized and encompasses mammalian NMDA and AMPA-like receptors, together with an invertebrate specific subgroup of glutamate gated chloride ion channels (11). The *C. elegans* genome encodes at least three mGluRs, designated *mgl-1*, *mgl-2* and *mgl-3*. Whilst the experimental tractability of *C. elegans* has provided insight into the molecular, cellular and functional organisation of the iGluR family (11), comparatively less is known about the function of the MGL class of receptor in *C. elegans*. The identification of mGluRs in invertebrates that are closely related to specific vertebrate mGluR subtypes suggests that this class of receptor may play a similarly important role in signalling and adaptive behaviour within simpler organisms (12-15).

C. elegans displays a number of rhythmic behaviours that undergo adaptation and are modulated by the activity of simple microcircuits, which integrate sensory information from both the worms' external and internal environment. A key sensory cue that governs the pattern of activity within these microcircuits is food (16,17). Indeed, both dopaminergic, cholinergic and 5-HT signalling via GPCRs has previously been shown to contribute to a number of food dependent behaviours, which encompass changes in patterns of locomotory sub-behaviours and pharyngeal function (18-20). Hence, the presentation and removal of a sensory cue, such as food, represents two very distinct contexts which change the worms' behaviour by separate signalling pathways. In *C. elegans* context-dependent signalling has been resolved at the level of neurons expressed within circuits that are responsible for either the detection of sensory cues or the integration of sensory signals with motor co-ordination. For example, the glutamatergic circuitry involved in chemotaxis towards an attractant contains both OFF-sensing neurons, which are active in the absence of an attractant and ON-sensing neurons that are active in the presence of an attractant. OFF and ON situations represent distinct contextual states and the co-ordinated signalling between OFF-sensing and ON-sensing neurons provides a mechanism by which *C. elegans* can initiate adaptive changes in behaviour in response to contextual changes such as the presentation and removal of a sensory cue (21). *C. elegans* feeding behaviour has previously been shown to change upon the presentation and removal of food (20,22), highlighting that circuits contributing to the activity of the pharynx are subject to context-dependent signalling. The observation that glutamate signalling can activate circuits to mimic feeding behaviour in the OFF-food state implicates a role for this neurotransmitter pathway in the context-dependent modulation of the pharyngeal nervous system[2]. Glutamatergic signalling and specific receptors therein may therefore contribute to the signalling pathways underlying context-dependent changes in *C. elegans* feeding behaviour.

Here we describe three metabotropic glutamate receptors that have a widespread expression in the nervous system of *C. elegans*. The *mgls* appear to be differentially expressed exclusively in the nervous system of *C. elegans*. *mgl-1*, *mgl-2* and *mgl-3* expression in the pharyngeal nervous system suggests their involvement in the modulation of pharyngeal network activity. Electrophysiological recordings on a semi-intact preparation of the *C. elegans* pharynx, combined with the use of mGluR agonists and worms with putative null

mutations identified that under these experimental conditions both *mgl-1* and *mgl-3*, but not *mgl-2*, can modulate the activity of the pharyngeal circuit. Experiments performed on intact animals suggest that of the three receptors *mgl-1* makes a significant contribution to changes in feeding behaviour upon acute food removal and to the context-dependent modulation of *C. elegans* feeding behaviour. Overall the results reveal a role for glutamate neurotransmission and MGL receptor signalling in context-dependent feeding behaviours.

EXPERIMENTAL PROCEDURES

Culturing of *C. elegans*

C. elegans strains were cultured under standard conditions (23). Wild-type Bristol N2 and *eat-4(ky5)* was obtained from the *Caenorhabditis Genetics Centre* (CGC). The strain *pha-1(e2123)* was obtained from R. Schnabel. The putative *mgl* knockout strains *mgl-1(tm1811)*, *mgl-2(tm0355)* and *mgl-3(tm1766)* were obtained from the National Bioresources Project (Tokyo women's Medical University, Tokyo), the *mgl* green fluorescent protein (GFP) reporter strain *utIs35[mgl-1::GFP]* is a *mgl-1::GFP* gene fusion under the *mgl-1* promoter (as described in *unpublished communication*[3]). The *mgl* mutant strains were out-crossed at least 3 times.

Molecular phylogeny of MGL proteins

Protein sequences for 77 metazoans with sequenced genomes were downloaded from Ensembl (Version 61; 3/2/11) (24). In addition, *Brugia malayi* proteins were downloaded from Wormbase (13/2/11) (25). Homologues of *C. elegans* MGL-2 (F45H11.4.2) were identified from these proteomes using BLAST (26) and the protein family constructed with HAQESAC (27). Protein alignments were performed with MAFFT (28), using default settings. Minimum evolution molecular phylogenies were constructed using FastTree (29) with 1000 bootstrap replicates.

RACE, SL-1 and Predictive PCR analysis

RACE (rapid amplification of cDNA ends) amplifications. Total RNA was extracted from mixed stage Bristol N2 animals using a TRIzol® (Invitrogen) extraction method. Both reverse transcribed mRNA and *C. elegans* cDNA library (Origene) were used as template for the various characterization techniques used and outlined below. All 5´-RACE products analysed in the present study derived from two rounds of amplification using a 5´-RACE primer in the first reaction and a nested 5´-RACE primer in the second reaction as indicated below. In contrast, all the analysed 3´-RACE products were generated using a single amplification with a 3´-RACE primer. For these experiments, 1 µg of total RNA was used to perform first-strand cDNA synthesis and incorporate either the 5´- or 3´-RACE adaptor sequence as described by the manufacturer (SMART RACE cDNA amplification kit; Clontech). The RACE adaptor fused first-strand cDNA was used directly as the template for RACE PCR. RACE primers were designed using the sequence information available at the time. The sequence of the primers used was as follows: *mgl-1* 5´-RACE (5´-GATGGCGAGCTCTCGTCATCTGTCATCCTC- 3´), *mgl-1* 5´-nested RACE (5´-GTCATTGTTTCTATCCCACGACTCTGATGCAAGC-3´), *mgl-1* 3´-RACE (5´-CTCCGCCTGGGTCAACGGCATCAAGGTGC-3´), *mgl-2* 5´-RACE (5´-CGATGCTGTTCGTGTGACTCCTCCACCCATAC-3´), *mgl-2* 5´-nested RACE (5´-GTCGGATAAGTCTGGAGTGGTGGCGGAG-3´), *mgl-2* 3´-RACE(5´-GTCGGAGTTGGTTTGATGCGGGATTGGCCGGATG-3´), *mgl-3* 5´-RACE(5´-GAACCGGAGGAATTGGCACGAAAAATGAAGAG-3´), *mgl-3* 5´-nested RACE (5´-CGGCTCCTGTTGAACTGTAGCTGACTTGAGG-3´) and *mgl-3* 3´-RACE (5´-GAATGGTGACGGAATCGGACGATATGATGTCTTC-3´).

C-terminal domain amplification

Mixed stage cDNA was used as a template in reactions designed to amplify the sequences encoding the entire intracellular C-terminal domain of the receptors. This was done with primers encoding the 5´ (5´-CT) end of this domain and 3´-end (3´-CT) encoding the last 8–10 amino acids preceding the predicted stop codon. *mgl-1* 5´-CT (5´-GAAAAACACAAAAACGTCCGAAAG-3´), *mgl-1* 3´-CT (5´-TCATAAGAAAGTATCGTGAGC-3´), *mgl-2* 5´-CT (5´-CATCCTGAGAAGAATATCAGA-3´), *mgl-2* 3´-CT (5´-TCAAAAGATTTGCTTGAAATC-3´), *mgl-3*

5´-CT (5´-CAACCATACAAAAATGTGAGG-3´) and *mgl-3* 3´-CT (5´-TCAAAGAAAAGTGGAATTAGTGTC-3´).

SL (splice leader) analysis

SL primers were designed according to the published sequences for SL-1 (splice leader-1) (5´-GGTTTAATTACCCAAGTTTGAG-3´) and SL-2 (splice leader-2) (5´-GGTTTTAACCCAGTTACTCAAG-3´) respectively. These were combined in a standard PCR reaction with *mgl-1*-5´-RACE and *mgl-3* 5´-nested RACE as required. All PCRs were performed with the enzyme BD Advantage2 (Clontech). 'Touchdown' PCR parameters were used for the first round RACE reaction; all other PCRs were performed under standard conditions (Clontech). The amplified fragments were gel-extracted (Qiagen) and ligated into a suitable vector before sequencing (MWG Biotech). The cDNA was aligned to *mgl* sequences using BLASTn (NCBI) and Wormbase.

Rescue experiments

The cosmid ZC506 was used to perform *mgl-1(tm1811)* rescue experiments and was supplied by the CGC. The cosmid ZC506 (at 10-15ng/µl) was co-injected with the *myo-2::GFP* reporter plasmid pPD11833 (obtained from A. Fire) at 20-30ng/µl. The expression of GFP in the pharyngeal muscle was used to screen for transgenic lines expressing ZC506.

Generation of the *Peat-4::ChR2;mRFP* integrated strain

ChR2 was amplified from the plasmid *Pmyo-3::ChR2(H134R);YFP* using the primers (F) 5'-CTAGAGACTAGTATGGATTATGGAGGGC CTG and (R) 5'-ATGGGGTACCTTAG GGCACCGCGCCAGCCTCGGCCTC. The (R) primer contained a synonymous substitution that removed a Kpn-I site internal to ChR2 and introduced an artificial stop codon. ChR2 was cloned Spe-I/Kpn-I upstream of mRFP in the gateway entry vector p-ENTR. This was recombined with the gateway destination vector, p-DEST., containing 6Kb of *eat-4* promoter to generate the construct *Peat-4::ChR2;mRFP*. The construct *Peat-4::ChR2;mRFP* was injected at a concentration of 50ng/µl. Lines were established from the F2 generation stably expressing *mRFP*. *Peat-4::ChR2;mRFP* was integrated by UV irradiation and outcrossed x6.

Construction of the *mgl-2::GFP* and *mgl-3::GFP* gene reporter

For the *mgl-2*::*GFP* reporter construct the primers 5'-CATGCATGCAAGCAAACTGAAAATCGCT CCGTGG and 5'-CAAGGTACCTTCGCCGCGTTTTTGCTCTT TTCTAC were used to amplify ~4.5Kb of *mgl-2* promoter, this was cloned into the fire vector pPD95-75 using the restriction sites Sph-1/Kpn-1. Using the primers 5'-GTTGGTACCAATGGTGTAGCTTGAGACA GC-3' and 5'-CAAGGTACCATGCTCTACAGTCATGTCAC AC-3' the full length cDNA encoding MGL-2 (F45H11.4 in WS243) was amplified, TOPO cloned (Invitrogen) and cut using the enzyme Kpn-I. The 5' Kpn-I site was incorporated into the 5' primer, whereas the 3' site was internal to the MGL-2 coding sequence and located within the C-terminal. This product was cloned downstream of the *mgl-2* promoter in the vector pPD95-75 using the Kpn-I restriction site to generate an MGL-2 protein fusion to GFP at the C-terminal. This was injected at 20ng/µl into the N2 strain by standard techniques (30).

For the *mgl-3::GFP* reporter construct the primers *5´-TTCGTCGACAATAGTATTCCCGAGAACGG and 5´-GCGGCCGCTTTTACTGTCGAACTGATTGG* were used to amplify ~5Kb of *mgl-3* promoter and the first exon (containing the first putative start codon). This fragment was cloned upstream of *GFP* in the vector pHAB*GFP* (provided by Howard Bayliss) using restriction sites Sal-I and Not-I to generate the construct *mgl-3::GFP*. This was co-injected at 10-20ng/ul with the *pha-1* rescue plasmid pBX (obtained from R. Schnabel) into the temperature sensitive strain *pha-1(e2123)* by standard techniques (30). Transformed lines were selected at temperature sensitive conditions (25.5^{o}C).

Imaging of the *mgl::GFP* reporter strains

Animals were mounted in a 5µl drop of 10mM levamisole (Sigma) on a 2% agarose pad covered with a 24x24mm coverslip. Differential interference contrast (DIC) and fluorescence imaging was performed on a Nikon Eclipse TE800 fluorescence microscope equipped with a Hamamatsu C4742-95 Digital Camera. Confocal

images were captured with a Zeiss LSM- 510 laser-scanning microscope.

Electropharyngeogram (EPG) Recordings

Hermaphrodite animals were grown on a bacterial lawn of OP50 and young adults were picked for electrophysiological experiments. Animals were placed into a Petri dish containing modified Dent's saline (composition in mM: Glucose 10, HEPES 5, NaCl 140, KCl 6, $CaCl_2$ 3, $MgCl_2$ 1 and pH7.4) supplemented with Bovine Serum Albumin (0.1% w/v). Worms were dissected by cutting them at the pharyngeal-intestinal valve with a razor blade, causing the cuticle to retract and exposing the isthmus and terminal bulb to generate a semi-intact pharyngeal preparation in which the pharyngeal microcircuit remains intact. The dissected preparation will have a distinct physiology to the intact organism, where the somatic nervous system is completely intact. All experiments were performed at room temperature (≈ 20-22^{o}C). The pharyngeal preparation was transferred to a custom made recording chamber (volume 1mL) mounted on a glass coverslip. Suction pipettes were pulled from borosillicate glass (glass diameter 1mm; tip diameter ≈12µm; Harvard Instruments). The pipette was lowered into the recording chamber and placed close to the anterior end of the preparation. Suction was then applied to attach the preparation to the pipette. The suction pipette was attached to an Axoclamp 2B recording amplifier. The reference electrode was a silver-chloride pellet in Dent's saline connected to the recording chamber by an agar bridge. Extracellular voltage recordings were made in "bridge" mode and the extracellular potential was set to 0 mV using the voltage off-set immediately prior to recording. Data was acquired using Axoscope (Axon Instruments) and stored for subsequent off-line analysis.

In single dose experiments the recordings were made from the pharynxes in Dent's saline for 5 min. The drug was then applied to the semi-intact pharyngeal preparation by removing and replacing the solution with a 1mL pipette. Recordings were made from the pharynx in the presence of drug for 5 min and then the drug was washed off. The frequency of the EPGs was measured for the 5 min before drug application and for 5 min after the drug application. The drug was then washed off the preparation. After the drug was washed off the preparation the EPGs were measured for a further 5 min in Dent's saline. Following the 5 min recovery period in Dent's saline 500nM 5-HT was applied by removing and replacing the Dent's with a 1ml pipette. EPGs were measured for a further 2½ min in the presence of 5-HT. The duration of the entire experiment for a single worm did not exceed 25 minutes, including the time taken to dissect the worm pharynx and apply the suction electrode.

The LCCG-I concentration response curve was generated by sequentially applying increasing concentrations of drug to the dissected semi-intact pharynxes. The addition of each concentration was preceded by a 5 min recovery period in Dent's saline. The drug was applied for 2.5 min and the EPGs were measured during this period. The effect of the drug on the frequency of pharyngeal EPGs is expressed as a percentage change compared to the basal resting rate during the 2½ min immediately before the addition of the drug. The duration of the entire experiment for a single worm did not exceed 77.5 minutes for *mgl-1*and 62.5 minutes for N2 including the time taken to dissect the worm pharynx and apply the suction electrode.

Intracellular Recordings

The dissected pharynx was transferred to a custom-built perfusion chamber, volume 1 mL, on a glass cover slip. The recording chamber was mounted on a microscope stage and perfused via gravity feed with saline at a rate of 20 mL min^{-1}. The preparation was secured with a glass suction pipette applied to the terminal bulb region of the pharynx and then impaled with an aluminosilicate glass microelectrode, 1.0 mm outer diameter pulled on a microelectrode puller to tip with resistance 60-80 MΩ, filled with 4 M potassium acetate and 10mM KCl, and connected to an Axoclamp 2A amplifier. The reference electrode was a silver chloride-coated silver pellet in 3M KCl connected to the recording chamber by an agar bridge. Data was acquired and analyzed using PClamp8 (Axon Instruments). Drug solutions were diluted with Dent's saline from stocks as required.

Electrophysiological recording of the *Peat-4::ChR2;mRFP* light evoked response

The strains N2;*Is[Peat-4::ChR2;mRFP], mgl-1(tm1811);Is[Peat-4::ChR2;mRFP]* and *eat-4(ky5);Is[Peat-4::ChR2;mRFP]* were subjected to pharyngeal dissection as in (31).

Desheathed pharynxes were placed in a recording chamber and illuminated using a blue LED, with wavelength 470nM (as described in (31)). Intracellular recordings of muscle action potentials were recorded from the terminal bulb using sharp electrodes (as described above). For N2;*Is[Peat-4::ChR2;mRFP]* and *mgl-1(tm1811);Is[Peat-4::ChR2;mRFP]* recordings were made in the presence and absence of LCCG-I. The last 10 light stimuli, for each phase of the experimental time course were analysed.

Chemicals

(±)-1-Aminocyclopentane-trans-1,3-dicarboxylic acid ((±)trans-ACPD) (Cat#0187), and (2S,1´S,2´S)-2-(Carboxycyclopropyl)glycine (LCCG-I) (Cat#0333) were obtained from Tocris Biosciences (Bristol, UK). All other chemicals were obtained from either Sigma or Fisher.

Pharyngeal Pumping Assays in Intact Animals

A synchronized population of young adult worms was generated by picking L4 staged animals to a fresh food plate 16-18 hours before performing the assay. For each individual animal the number of pumps performed within 1 minute on food was counted, the food was then removed by placing the animal onto a fresh non-food plate and allowing it to move around for 1 minute. Individual animals were each transferred to a separate, second non-food plate and the number of pumps (defined as the number of backwards movements of the terminal bulb grinder) performed in 1 min was counted at two time points, 5 min and 95 min following the transferral. Then after 96 min worms were returned to food and at 100 min the pharyngeal pumping was recorded.

Data Analysis

The results are expressed as the percentage change in frequency ± s.e.m of the mean for *n* individual pharynxes. For the EPG recordings each drug was tested on a separate pharynx. Significance was measured using one-way ANOVA, with Bonferroni post-test, unless otherwise stated. Concentration-response curves were plotted by fitting the data to the modified logistic equation (GraphPad Prism, San Diego, CA), and EC_{50} values are given with 95% confidence limits.

RESULTS

Molecular organization of MGL subtypes

A combination of PCR-mediated approaches (RACE, SL-1/2 amplifications and predictive PCR; *see methods* for further details) were applied to either of two cDNA pools independently prepared from mixed stage animals (*see methods*) to characterize the 5′ and 3′ ends of the *mgl* cDNAs. The combined findings of these different approaches is published elsewhere (32) and are presented in summary here, together with a revised annotation for *mgl-2* based upon further analysis. The *mgl-1* gene encodes at least 3 different 5′ isoforms two of which are alternatively trans-spliced to SL-1, the nematode specific trans-splice leader. One of the SL-1 trans-spliced variants supports the 5’ gene structure currently defined for *ZC506.4b*. The other SL-1 trans-spliced variant (European Nucleotide Archive Accession#: LN681209) and 5’RACE analysis (European Nucleotide Archive Accession#: LN681208) identified alternative 5’ gene structure (Figure 1). The sequence of the putative signal peptide predicted from the translated 5′ cDNA sequences of each of the *mgl-1* isoforms suggests that each of the 5’ variants use the same ATG as their start codon. The 3’RACE amplification identified a single *mgl-1* C-terminal variant and redefines exon 11 of *ZC506.4b* (European Nucleotide Archive Accession#: LN681210) (Figure 1).

A single *mgl-2* 5′ isoform was identified that was not trans-spliced to SL-1 sequence (attempts to amplify *mgl-2* 5′ cDNA using SL-1 and SL-2 complementary primers were unsuccessful). The 3′ cDNA analysis suggests *mgl-2* encodes at least two different 3′ isoforms. Predictive PCR identified that alternative splicing creates a long and a short C-terminal variant (denoted *mgl-2i* and *mgl-2ii* respectively). The long C-terminal variant (*mgl-2i*) corresponds to the transcript currently defined in Wormbase (transcript F45H11.4, Wormbase version WS243). The 3′ RACE analysis covered an extended region of the *mgl-2* gene compared to the predictive PCR and confirmed the alternative splicing in *mgl-2ii* (Figure 1). In our analysis we identified the ORF of *mgl-2ii* and the downstream gene, *maf-1* were contained within a single transcript. This was confirmed by the amplification of a single transcript using primers designed against the *maf-1* 3’ end and *mgl-2* 5’UTR. Sequencing of this transcript confirmed both the alternative

splicing in *mgl-2ii* and a 4 nucleotide overlap (ATGA) between the 3' end of *mgl-2ii* and the 5' end of *maf-1*, which contains the putative TGA stop codon for *mgl-2ii* and the putative ATG start codon for *maf-1* (European Nucleotide Archive Accession#: LN681207). The ORF of *mgl-2ii* and *maf-1* were not in-frame with each other and *in-silico* translation in their respective reading frames each gave rise to bona-fide protein sequence.

At least two different *mgl-3* 5′ isoforms were identified, the difference being that one variant was SL-1 trans-spliced (European Nucleotide Archive Accession#: LN681212), whilst the other contained a predicted untranslated exon within the 5′ promoter region, located ≈15Kb upstream of the first coding exon (European Nucleotide Archive Accession#: LN681211) (Figure 1). The analysis of the C-terminal of *mgl*-3 suggests that it undergoes alternative splicing, giving rise to at least three different C-terminal splice variants (*mgl-3i/ii/iii*) (Figure 1). In *mgl-3ii* (European Nucleotide Archive Accession#: LN681214). exon 16 uses an alternative splice donor site to *mgl-3i/iii* that incorporates 6 additional nucleotides that are otherwise intronic in *mgl-3i* (European Nucleotide Archive Accession#: LN681213). and *mgl-3iii* (European Nucleotide Archive Accession#: LN681215).The result of this is the substitution of a threonine residue for the amino acid triplicate IleSerAla. Other than this the sequence of the *mgl-3i/ii* 3′ cDNA region that was PCR amplified was the same. In *mgl-3iii* alternative splicing caused a frame-shift in the downstream open reading frame and the introduction of an alternative stop codon. The isoform *mgl-3iii* has been independently identified by the EST submission EC001043. The 3' RACE analysis of the *mgl-3* C-terminal confirmed the *mgl-3i* splice variant (European Nucleotide Archive Accession#: LN681216).

The molecular phylogeny of the MGR family provided in this study is an updated analysis and a further clarification of that previously published in (32). It supports the assignment of the three nematode MGL proteins to the three mammalian MGR types (Figure 2). MGL-2 forms a well-supported clade with vertebrate Group I (>99% bootstrap support). MGL-1 has previously been classified weakly as Group I-like (32,33) but phylogenetic analysis (and BLASTP results) show that it is actually more closely related to vertebrate Group II sequences (>97% bootstrap support). MGL-3 is most similar to Group III sequences (Figure 2; >80% bootstrap support). Although none of the insect species with fully sequenced genomes to date have all of the MGR types, sequences from different insects indicate that there may be four subfamilies. mGluRB (FBpp0271833) (also known as DmXR or mangetout), is not a glutamate receptor, however, and it has been suggested that it has diverged from the rest of the family to recognise a different ligand that is not a natural amino acid (34). It is not known whether the sea urchin orthologue (SPU_017426tr) is recognised by glutamate but the topology and presence of four echinoderm GluR sequences is consistent with this "Group X" subfamily being lost in the chordate lineage, rather than gained in the insect lineage. Although not conclusive, this analysis suggests that Group X is most closely related to Group III (77% bootstrap support). Consistent with previous studies in *C. elegans*, none of the fully sequenced nematodes analysed had a Group X receptor.

Distinct and overlapping expression patterns for the 3 *mgl*s in *C. elegans*

To assess and compare the expression patterns of each of the three *mgls* in *C. elegans* transgenic animals, expressing extrachromosomal fusions to GFP, were constructed for *mgl-2* and *mgl-3 (see methods)*. For *mgl-1* a gene fusion to GFP was independently generated (*see methods*) and analysis was performed on animals stably expressing the *mgl-1::GFP* as an integrated array. Of the three receptors, *mgl-1* appeared to have the most widespread expression pattern. The reporter *mgl-1::GFP* was extensively expressed in the nerve-ring, in tail neurons and extensively within the pharyngeal nervous system, which included the neurosecretory motorneuron NSML/R, interneurons and motorneurons (Figure 3 A –C). In worms expressing *mgl-2::GFP* as an extra-chromosomal array GFP fluorescence was identified in the nerve ring, tail neurons and the pharyngeal nervous system, where it was expressed in NSML/R (Figure 3 D-F). The analysis of *mgl-2::GFP* transgenic lines also identified GFP expression in the glutamatergic pharyngeal neuron I5, anterior and posterior intestine, pharyngeal-intestinal valve and pharyngeal muscle. However, the expression of

GFP in these tissues was not consistent between transgenic lines analysed. In worms expressing *mgl-3::GFP* as an extra-chromosomal array GFP fluorescence was detected in the pharyngeal nervous system, specifically NSML/R and in the nerve ring (Figure 3G).

Pharmacological characterization of *mgls* using EPG recording in the pharynx

To further investigate if *mgl* receptors control pharyngeal pumping an electrophysiological assay was developed using mGluR agonists that have a well characterized efficacy at mammalian mGluRs (35) and have previously been shown to exert activity on invertebrate nervous systems (14,15).

The electropharyngeogram (EPG) is an extracellular recording technique that enables the detection of electrical transients in the pharyngeal muscle and associated circuit of 20 neurons, which are embedded underneath the basement membrane. The myogenic activity of the pharyngeal muscle is modulated by the activity of the pharyngeal nervous system (36). In the experiments described here an incision is made at the pharyngeal-intestinal valve leading to the extrapharyngeal nervous system being displaced (Figure 4A) and leaving the embedded pharyngeal neurons which express *mgl-1, mgl-2* and *mgl*-3. This ensures that the drug response is driven either by the action of receptors expressed in pharyngeal neurons or by direct activation of the underlying pharyngeal muscle.

EPG recordings were made from wild-type animals to look at the effect of mammalian mGluR agonists on the electrophysiology and pumping behaviour of the pharynx (Figure 4). (±)trans-ACPD is a mammalian mGluR agonist with broad spectrum activity against the distinct sub classes of receptor (35). Pharmacological profiling of representative mGluR group members suggests (±)trans-ACPD is a potent agonist of Group I (EC_{50}= 15μM at mGluR1) and Group II receptors (EC_{50}= 2μM at mGluR2) and a weak agonist at Group III receptors (EC_{50}=800μM at mGluR4)(35).

Initially 100μM (±)trans-ACPD was applied to the wild-type preparation. (±)trans-ACPD is an equimolecular mixture of (1S,3R)- and (1R,3S)-ACPD and a selective agonist for mGluRs. A variable response was obtained that consisted of a large increase, no change or an inhibition of the basal pumping frequency (*data not shown*). At the increased concentration of 500μM, which is more in keeping with the EC_{50} of this agonist at Group III mGluRs, (±)trans-ACPD consistently caused a reversible inhibition of basal pumping in wild-type pharynxes (Figure 4B). In a high proportion of animals a rebound excitation was recorded during the first few minutes of the recovery period, after the drug was washed off (Figure 4B). The neurotransmitter 5-HT is known to be a potent stimulator of pharyngeal pumping ***(37,38)***. Following the wash period 500nM 5-HT was applied to assess the viability of the pharynx at the end of the recordings. In each recording the application of 500nM 5-HT caused a potent stimulation of pharyngeal pumping, confirming the pharyngeal circuit was still capable of high frequency pumping after (±)trans-ACPD had been applied and following a 5 minute wash period (Figure 4B). LCCG-I is a more potent broad spectrum mGluR agonist than (±)trans-ACPD and has a higher potency at mGluR II and III subgroups. The EC_{50} at representative Group I, II and III mGluRs is 50μM (mGluR1a), 1μM (mGluR3) and 9-50μM (mGluR4a) respectively (35). The application of 100μM LCCG-I to the wild-type pharynx preparation caused a consistent and reversible inhibition of the EPGs which was often complete for the period of drug exposure (Figure 4C). For the same reasons as previously described, 500nM 5-HT was applied to the pharynx after LCCG-I had been applied and after a 5 minute wash period. In each recording the application of 500nM 5-HT caused a potent stimulation of pharyngeal pumping, confirming the pharyngeal circuit was still viable and retained the sensitivity to 5-HT. The EC_{50} for the inhibition of pharyngeal pumping by LCCG-I was measured at 3μM in the dose response analysis (Figure 4D).

The intracellular recording configuration enables the measurement of pharyngeal muscle activity (Figure 4E). Compared to the EPG, it provides a more direct measure of pharyngeal pumping and its modulation by the embedded pharyngeal nervous system. In such recordings 10μM LCCG-I caused an inhibition of spontaneous action potential firing however the resting membrane potential (-75mV) was not changed by the addition of the drug (Figure 4F). The latter supports the expression studies that failed to detect receptors in the muscle arguing against a direct effect of LCCG-I on this tissue. Rather the intracellular recordings indicate that

LCCG-I activates receptors that reside within the pharyngeal nervous system and modify network activity that supports pharyngeal pumping. The potency of LCCG-I (EC_{50} 3μM) suggest a specificity at the Group II like *mgl* receptor (*mgl-1*) but we extended the analysis to investigate pharmacological activation by LCCG-I in the various *mgl* mutants.

LCCG-I modulation of network activity across *mgl* mutants

Deletion alleles exist for each of the three *mgl* receptors; these are *mgl-1(tm1811)*, *mgl-2(tm0355)* and *mgl-3(1766)*. The mutations were confirmed by PCR using both genomic DNA and cDNA derived from the *mgl* mutants. DNA sequencing of the amplified PCR products confirmed that in each case the deletion culminates in a putative null (*data not shown*).

To probe the basis of the mGluR agonist activity in the wild-type pharyngeal preparation EPGs were conducted on the *mgl* mutants in the presence of each agonist. (±)trans-ACPD was only tested on *mgl-1(tm1811)* at 500μM and pumping by these animals was not impaired as in the wild-type, by the drug (*data not shown*). LCCG-I was tested over a range of concentrations on each of the *mgl* mutants (Figure 5A, B and C). EPGs by *mgl-1(tm1811)* animals were not inhibited over the range 1-12.5μM, but at the higher concentrations tested (25μM and 100μM) a partial inhibition began to be observed (Figure 5D). In contrast to *mgl-1(tm1811)*, both *mgl-2(tm0355)* and *mgl-3(tm1766)* EPGs were strongly inhibited by concentrations of LCCG-I at 3μM and 10μM (Figure 5E), suggesting *mgl-1* is primarily responsible for the LCCG-I response. The wild-type response of pharynxes to LCCG-I was restored in *mgl-1(tm1811)* by injecting cosmid DNA (10-15ng/μL) (Fig 5D) containing the entire *mgl-1* genomic sequence and ≈3.6Kb of sequence upstream of the first non-coding exon defined by RACE analysis (Figure 1). This provides further support for the hypothesis that *mgl-1* is responsible for the inhibitory effect of LCCG-I on the pharynx.

At the lower range of LCCG-I concentrations tested (1μM) an increase in the frequency of EPGs was measured from both *mgl-1(tm1811)* and *mgl-2(tm0355)* (Figure 5D and 5E respectively), but not *mgl-3(tm1766)*. Instead *mgl-3(tm1766)* was inhibited by LCCG-I without the low dose activation seen at 1μM (Fig. 5E). Thus, *mgl-3* appears to increase the frequency of pharyngeal pumping at low concentration. The modulation of the pharyngeal network in an *mgl-1* and *mgl-3* dependent manner further supports the expression of these receptor subtypes within this microcircuit.

Optogenetic activation of glutamatergic evoked activity in the pharyngeal network is modulated by LCCG-I.

Next we wanted to identify if the presynaptic activation of *mgl-1* within the pharyngeal nervous system inhibited glutamate initiated changes in the activity of the postsynaptic pharyngeal muscle. Optogenetics enables the discrete activation of specific subsets of neurons within a network. Hence, an optogenetic approach was used to selectively depolarise neurons capable of glutamate release within this network. Light evoked changes in the activity of the pharyngeal network were measured by making simultaneous intracellular recordings from the pharyngeal muscle, which is the postsynaptic target of the pharyngeal neural network. This optogenetic electrophysiological approach was combined with the pharmacological activation of *mgl-1* using the agonist LCCG-I.

The optogenetic depolarisation of glutamatergic neurons was achieved by using an integrated line in which the light sensitive channel rhodopsin (ChR2) was expressed under the control of the *eat-4* vesicular glutamate transporter promoter (*Peat-4::ChR2;mRFP*). The expression of this construct is wide spread in the *C. elegans* nervous system but restricted to M3, NSM, I2 and I5 in the pharynx[1], consistent with its expression in the glutamatergic neurons. Worms were cultured on NGM plates containing retinal, an essential co-factor required for ChR2 activation. A 1 msec pulse of light (470nm) did not excite the exposed pharynx of N2 worms that had not been transformed with *Peat-4::ChR2;mRFP* (Figure 6A) and (31). Light activation of the exposed pharynx of wild-type worms expressing *Peat-4::ChR2;mRFP* produced a tightly coupled light evoked excitation in the pharyngeal muscle (Figure 6B). The light activated response is initiated from the glutamatergic neurons of the circuit however the evoked response measured at the muscle involves a complex depolarization usually followed by a superimposed action potential. The

complexity of the response arises because the pharyngeal glutamatergic neurons produce activity in the circuit via gap junctions and the release of transmitters in addition to glutamate. These interactions are the major determinant of the complex response that is recorded in the muscle ((31) and unpublished observation[1]). This expected observation is reinforced by the fact that although the light induced response is delayed it is not prevented when it is triggered in the pharynx of *eat-4* mutant animals that lack glutamate release but retain other activities independent of glutamate release (Figure 6B and 6C)

To determine if *mgl-1* inhibits the light activated response the optogenetic electrophysiological experiments were combined with the pharmacological activation of *mgl-1*. 10μM LCCG-I was bath applied and light evoked recordings were made from the exposed pharynx of wild-type worms expressing *Peat-4::ChR2;mRFP*. As in the previous pharmacological experiments that used intrinsic activity, the application of LCCG-I at a dose (10μM) that is selective for the *mgl-1* mediated inhibition caused a reduction in the percentage of the light evoked pharyngeal muscle depolarization (Figure 7A and 7B). This LCCG-I inhibition of the light evoked pharyngeal depolarization was reversed upon washout. The LCCG-I often reduced the rise of the light induced response but the complex nature of this initial depolarization limits the use of this parameter as a measure of the drug effect. In contrast the inhibition by LCCG-I was clearly quantified by comparing the almost complete inhibition of the light evoked pharyngeal action potentials that were otherwise frequently seen when light activation was performed in the absence of the drug (Figure 7A and 7B). The inhibition of the light evoked pharyngeal muscle response by LCCG-I was reversed to almost wild-type levels during the wash phase (the basal and wash periods were not significantly different in a paired Student's t-test).

Light evoked recordings were then made from the exposed pharynx of *mgl-1* worms expressing *Peat-4::ChR2;mRFP*, in the absence and presence of LCCG-I. The percentage of stimuli that evoked a full action potential in the absence of LCCG-I during the basal period and then in the presence of 10μM LCCG-I was not significantly different in the *mgl-1(tm1811)* mutant background (Figure 7C). This suggests that *mgl-1* activation is largely responsible for the LCCG-I mediated inhibition of light evoked changes in the network activity.

Modification of modulatory tone associated with an adaptive response to food deprivation in intact animals lacking *mgl* subtypes

The pharmacological detection of *mgl-1* as an inhibitor of pharyngeal pumping suggests it may be involved in the modulation of *C. elegans* feeding behaviour. Experiments in the isolated pharynx and whole organism represent a significant transition from an *in vitro* to an *in vivo* analysis. The modulation of the activity in the isolated pharynx is largely restricted to the embedded pharyngeal nervous system, whereas the intact worm will be subjected to additional extrapharyngeal regulation in response to changes in the external environment. We note that the *mgl-1* mediated inhibition of pharyngeal tone acts at the level of the intrinsic network activity, a situation that closely mimics when the worm is in an OFF-food state. Hence, we designed the whole organism assay around comparisons of the worm pharyngeal pumping both on and off food. As we have described a shift in the tone of the pharyngeal pumping in whole worms kept for an increasing period of time off food[2] we conducted off food measurements at 5 and 95 minutes. To this end we used pharyngeal pumping in the presence of food and its response to food deprivation as a tractable way to probe for a functional correlate of the drug mediated effect.We extended this to investigate wild-type animals and compared this to *mgl-1(tm1811)* animals. In addition the single mutant's *mgl-2(tm0355)*, *mgl-3(tm1766)* and the double mutant *mgl-1(tm1811);mgl-3(tm1766)* were included in the analysis to allow us to probe for functional evidence of the receptor interactions revealed in the semi-intact investigation of drug mediated *mgl* activation. Although *mgl-2(tm0355)* did not display a phenotype in the LCCG-I EPG, the expression of *mgl-2* in the pharyngeal circuit suggests that it may modulate pharyngeal function and so it was included in the analysis.

To investigate if the *mgl* receptors are involved in the food adaptive response a paired analysis was performed on animals in the presence of food and after being deprived of food for a short and extended period of time.

Pumping was counted for 1 minute at four time points, which were 0 min, where the animal is in the presence of food, 5 and 95 minutes after being transferred to a no-food environment. Worms were then returned to a food lawn and the pharyngeal pumping rate was counted at 100 minutes (Figure 8A).

The wild-type worms displayed context-dependent changes in the frequency of pharyngeal pumping. Initially a high frequency of pumping was recorded in the presence of food (268.4 ±3.7 s.e.m). This decreased after 5 minutes off food and underwent a time-dependent increase after being off food for 95 minutes. When placed back on food the pumping rate increased towards the high pumping rate initially recorded on food, however, it did not completely recover (Figure 8B). In the presence of food the pumping rate of single and double *mgl* mutants was not significantly different to wild-type (Figure 8B). After being food deprived for 5 minutes the pumping rate of wild-type animals on a no food arena was reduced to 10.85 ±3.23 (s.e.m) pumps min^{-1} (Figure 8B). After the same treatment the pump rate of *mgl-1(tm1811)* was significantly higher than N2, 29.11 ±6.09 pumps min^{-1} ($p<0.05$). The pump rate of *mgl-2(tm0355)* was increased compared to N2 but not significantly different. *mgl-3(tm1766)* pump rate was very similar to wild-type and not significantly different. This would suggest *mgl-1* is active during processes that create the acute inhibition of pharyngeal pumping in response to food removal. The *mgl-3* mutants did not exhibit this loss of inhibitory tone. This observation is consistent with the EPG recordings made from *mgl-3* mutants which suggest this receptor subtype excites pharyngeal pumping in the presence of a low concentration of LCCG-I. In addition the pump rate of the double mutant *mgl-1(tm1811);mgl-3(tm1766)* was not significantly different to the wild-type after 5min of food removal. This adds further support to the hypothesis that *mgl-1* and *mgl-3* activation has opposing effects on the activity of the pharyngeal nervous system, where *mgl-1* is inhibitory and *mgl-3* is excitatory. Following an extended period of food removal (95min) the pharyngeal pumping rate of the wild-type increased to 53.68 ±8 pumps min^{-1} (Figure 8B). All of the *mgl* mutants tested exhibited an increased pharyngeal pumping rate after 95min relative to counts made at 5 minutes off food. None of the rates recorded were significantly different to the wild-type. When wild-type worms were returned to food after being starved for 95 minutes the pharyngeal pump rate increased, approaching that initially recorded on food. The recovery of the *mgl* mutant strains was not significantly different to wild-type worms (Figure 8B). The rate of *mgl-3* pumping and *mgl-1(tm1811);mgl-3(tm1766)* pumping was not significantly different to the wild-type on food at the beginning of the experiment, after 95min off food and when returned to food.

The analysis of context-dependent behaviour would suggest the loss of *mgl-1* function has the greatest impact upon the acute response to food removal**.** To confirm the role of *mgl-1* in the acute response to food removal, the pumping rate of the rescue strain *mgl-1(tm1811)*;ZC506 was measured after 5 min of food removal and compared to *mgl-1(tm1811)* and wild-type strains (Figure 8C). The rate of pumping of *mgl-1* was significantly higher than N2, confirming the previous finding. The pumping rate of *mgl-1(tm1811)*;ZC506 was not significantly different to N2. This further supports the role for glutamate in the negative regulation of pharyngeal behaviour in response to acute food removal in the whole worm. In addition it highlights the contribution made by *mgl-1* in setting the inhibitory tone in response to changes in environmental sensory cues and the role of this receptor in modulating the activity of the pharyngeal neural network.

Discussion

The *mgl*s: a conserved arm of glutamatergic transmission in *C. elegans*

Three receptors with the domain organization associated with mGluRs are annotated in Wormbase. Our characterization of the cDNAs was used to better define the coding sequence of the annotated genes. When the three *mgl*s were compared they showed as much homology to each other as they did to the most related mammalian mGluRs, arguing that they make up a family of receptors encompassing three distinct sub-types. This molecular organization thus mirrors the situation that prevails in the vertebrate nervous system where molecular ontogeny into Group I, II and III is supported by selective pharmacological specificity and downstream signalling. The significance of this is that the identified molecular diversity of the *mgl*s suggests they

have similar potential to diversify signalling output from glutamate transmission. It is particularly striking that proteins encoding these receptors have many of the motifs that impart functional regulation at the level of receptor phosphorylation and scaffolding that are known to further diversify the complexity of mGluR signalling (39).

Molecular complexity to extend receptor diversity

Performing 5' and 3' RACE on the predicted gene sequences allowed us to resolve apparently unappreciated complexity in the promoter elements and splice variants within coding sequences that can be derived from the gene locus of *mgl-1*, *mgl-2* and *mgl-3*. In the case of gene control our analysis provided more precise transcription start sites many of which were authenticated by presence of SL1 splice leader sequences. This is true for *mgl-1*, *mgl-2* and *mgl-3*. In the latter case the RACE revealed the existence of a large 5' intron that interrupted an upstream non-coding exon in the 5' end of the gene. This variant was robustly amplified but was not preceded by a splice leader and there is no intervening gene in this region. The amplification of a single transcript, containing the open reading frame for both *mgl-2* and the transcription factor *maf-1* further highlights an apparent complexity of *mgl* function. The functional relevance of this finding is unclear; however it exemplifies the wider theme that there is potential for selective elements to control the developmental, temporal and spatial expression of the receptors.

Widespread and complimentary expression of *mgl*s

We used available GFP reporter strains to visualize the expression of *mgl-1* and complemented this with constructs designed to look at *mgl-2* and *mgl-3* expression. These reporters encompass many key determinants of the likely promoter regions and should provide rather faithful expression thus suggesting these receptors are restricted to the nervous system. Nevertheless the potential for further important expression beyond that documented by these reporters cannot be ruled out, particularly when as in the *mgl-3* genes there are clearly relatively complex promoter sequences. The expression patterns were relatively distinct and all cases seemed restricted to the nervous system. *mgl-1*, *mgl-2* and *mgl-3* were expressed in the nerve ring and they were also expressed in tail neurons.

mgl-1, *mgl-2* and *mgl-3* expression patterns appeared distinct but there was overlap in the case of the pharyngeal nervous system. This represents a microcircuit of 20 neurons that release a cocktail of fast transmitters and neuromodulators that regulate pharyngeal pumping. Striking in this was the clear overlapping expression of *mgl-1*, *mgl-2* and *mgl-3* in NSM the neurosecretory neuron that expresses the stimulatory modulator 5-HT. This expression suggested the potential co-ordinated use of these receptors in regulation of the pharynx. Although NSM is a classic neurosecretory 5-HT releasing neuron it additionally expresses the vesicular glutamate transporter, suggesting the potential to release glutamate (40) and other neuropeptide modulators (41). Although the expression of these *mgl*s in a glutamate releasing neuron would support a role as auto receptors the wide expression in particularly of *mgl-1* highlights their potential to act as both pre and postsynaptic detectors of glutamate. As detailed by comparison of ours (Figure 3) and others (42,43) the expression of *mgl-1* and *mgl-3* extends to a number of non-glutamatergic neurons suggesting broad potential in regulation of the neuronal pharyngeal microcircuit.

Pharmacological dissection of MGL function

The expression of *mgl-1*, *mgl-2* and *mgl-3* in the pharynx lent itself to the functional investigation of these receptors. None of the *mgl* mutants exhibited a discernible change in their pumping per se when measured using extrapharyngeal recording of the EPG. In contrast activation with two distinct mGluR agonists, known to activate invertebrate receptors (12,14), produced a dose dependent inhibition of pharyngeal function. Importantly, this major inhibitory effect was lost in the *mgl-1* mutants and suggests that these agonists lead to functionally coupled *mgl-1* receptor activation. LCCG-I effects were not impacted in the *mgl-2* mutant, suggesting that this receptor subtype does not contribute to the agonist mediated inhibition of pharyngeal pumping. The appearance of an excitatory effect of LCCG-I that otherwise inhibits, in the *mgl-1* mutants, suggests a cross talk with *mgl-3*. This could arise through one cell as both receptors are expressed

in NSM where *mgl-1* could inhibit and *mgl-3* promotes stimulatory output of this cell. This could be readily achieved by each receptor having distinct downstream signalling despite their shared activation by a common agonist; glutamate. This situation is aped in the sensory pathway of the worm at the level of ionotropic receptor signalling (21). An alternative explanation could be that this effect relates to differential activation of cells that selectively express the receptors. A striking feature of the *mgl-1* mediated LCCG-1 effects is that it leads to a complete but reversible inhibition of pharyngeal pumping. One might predict that in a structure like the pharynx, which is myogenic (36), that it would be difficult to achieve this with an agonist that indirectly modulates the muscle by neurogenic control. The intracellular recordings did not identify a direct effect of the *mgl* agonist on the muscle consistent with an indirect effect. A rebound response was observed upon removal of the agonist during the washout period. Indeed, such a phenomenon has been identified as a physiologically relevant way of imparting control within important sensory pathways including those that signal to higher function. In such scenarios the reduction of agonist activity can act as a stimulation of network activity (44). Such modulation may allow for excitatory signalling in a network, as *mgl* mediated inhibition is tonicaly changed in response to chronic changes in circulating glutamate. In the context of the pharynx this could derive from synaptically released glutamate but the pharyngeal neurons are well placed to sense changing concentrations of metabolites in the pseudocoelomic fluid. In this regard it is interesting to note that chronic effects of *mgl-1* and *mgl-2* have been noted with respect to starvation responses (42). This along with their conserved role as taste and gustatory receptors opens up the potential of pharyngeal receptors to co-ordinate nutritional cues as well as participating through more classical synaptic activation.

In a reverberating circuit in which one assays the network activity it can be difficult to resolve the precise locus of receptor mediated inhibition. Indeed, the widespread expression of *mgl-1* suggests a broad potential for receptor activation to act in glutamate releasing/sensing neurons. This is borne out by our experiments in which we selectively activated the circuit by light stimulation of the glutamate releasing neurons. This approach resolves a highly coupled muscle depolarization which involves a post stimulation depolarization with a superimposed action potential. The initial event is largely dependent on glutamate but appears not to be selectively effected by LCCG-1 mediated *mgl-1* activation. In contrast there is a more complete inhibition of the super imposed action potential which is driven by glutamate release onto the muscle and additional synaptically driven glutamate events that in turn drive cholinergic release in the pharyngeal microcircuits. This suggests that *mgl-1* could potentially act at several loci in the pharyngeal microcircuit and cell specific rescue of *mgl-1* function would be required to determine if this is an evenly distributed network effect or derives from a more discrete determinant.

Regulation of pharyngeal function and beyond

The analysis of *mgl* function in the pharynx has the virtue of allowing a combination of mutants and pharmacological investigation of function. However, this preparation failed to resolve a clear difference in the wild-type and mutants pharynx with respect to their un-stimulated pumping. For this reason we tested the pharyngeal response in the intact animal with respect to distinct food stimulation.

However, as indicated in the pharmacological experiments *mgl-1* activation produces a potent inhibition of pumping. Thus one might predict this receptor mutant would display an exaggerated response to food. This simple view neglects the possibility that the pharyngeal nervous system is additionally providing an integrated control of the pharynx in the absence of food. This is reinforced by the observations in the sensory systems detailing acute response to mimics of food removal (21). With this in mind we investigated pharyngeal pumping on food and at two time points after removal from food. These data in the wildtype recapitulate observations that suggest that after food removal worms stop pumping and slowly increase this for up to 90 mins ((45) and *unpublished observation*[2]). Observations that receptor activation by modulators and neuropeptides inhibits pumping and the data reported in this study suggest that the pharynx and its embedded microcircuit allows for an intricate balance in tone. Mutants that exhibit an exaggerated pumping in response to food

withdrawal suggest there is a loss of this tone. The observation that *mgl-1* mutants belong to this class suggests that they function in such a way and is consistent with the observation that pharmacological activation of the receptor leads to an inhibition of pharyngeal function. The expression pattern of *mgl-1* and the tractable effect of mGluR agonists in the isolated pharyngeal preparations suggest that *mgl-1* could exert such an effect at the level of the circuit within the intact organism. The exaggerated pumping phenotype of *mgl-1* was restricted to early time-points, following acute food removal and the elevated pumping after a prolonged period off food was equivalent in all mutant backgrounds. These observations highlight the selective contribution of *mgl-1* at a discrete time-point of an adaptive response.

Overall our observations highlight a powerful effect of *mgl-1* in the modulation of pharyngeal pumping behaviour. The modulation revealed by pharmacological investigations is reinforced by behavioural investigations and suggest a wider significance of *mgl* mediated signalling. As highlighted by the molecular diversity of *C. elegans mgl* subtypes this mode of glutamate signalling already exhibits significant complexity. Thus, *C. elegans* can model fundamental aspects of the key processes by which these receptors underpin function in higher organisms.

REFERENCES

1. Watkins, J. C., Davies, J., Evans, R. H., Francis, A. A., and Jones, A. W. (1981) Pharmacology of receptors for excitatory amino acids. *Adv Biochem Psychopharmacol* **27**, 263-273
2. Pin, J. P., and Duvoisin, R. (1995) The metabotropic glutamate receptors: structure and functions. *Neuropharmacology* **34**, 1-26
3. Awad, H., Hubert, G. W., Smith, Y., Levey, A. I., and Conn, P. J. (2000) Activation of metabotropic glutamate receptor 5 has direct excitatory effects and potentiates NMDA receptor currents in neurons of the subthalamic nucleus. *J Neurosci* **20**, 7871-7879
4. Heidinger, V., Manzerra, P., Wang, X. Q., Strasser, U., Yu, S. P., Choi, D. W., and Behrens, M. M. (2002) Metabotropic glutamate receptor 1-induced upregulation of NMDA receptor current: mediation through the Pyk2/Src-family kinase pathway in cortical neurons. *J Neurosci* **22**, 5452-5461
5. Herman, E. J., Bubser, M., Conn, P. J., and Jones, C. K. (2012) Metabotropic glutamate receptors for new treatments in schizophrenia. *Handb Exp Pharmacol*, 297-365
6. Oberman, L. M. (2012) mGluR antagonists and GABA agonists as novel pharmacological agents for the treatment of autism spectrum disorders. *Expert Opin Investig Drugs* **21**, 1819-1825
7. Yizhar, O., Fenno, L. E., Prigge, M., Schneider, F., Davidson, T. J., O'Shea, D. J., Sohal, V. S., Goshen, I., Finkelstein, J., Paz, J. T., Stehfest, K., Fudim, R., Ramakrishnan, C., Huguenard, J. R., Hegemann, P., and Deisseroth, K. (2011) Neocortical excitation/inhibition balance in information processing and social dysfunction. *Nature* **477**, 171-178
8. Rubenstein, J. L., and Merzenich, M. M. (2003) Model of autism: increased ratio of excitation/inhibition in key neural systems. *Genes Brain Behav* **2**, 255-267
9. Kehrer, C., Maziashvili, N., Dugladze, T., and Gloveli, T. (2008) Altered Excitatory-Inhibitory Balance in the NMDA-Hypofunction Model of Schizophrenia. *Front Mol Neurosci* **1**, 6
10. Conn, P. J., and Jones, C. K. (2009) Promise of mGluR2/3 activators in psychiatry. *Neuropsychopharmacology* **34**, 248-249

11. Brockie, P. J., and Maricq, A. V. (2006) Ionotropic glutamate receptors: genetics, behavior and electrophysiology. *WormBook*, 1-16
12. Parmentier, M. L., Pin, J. P., Bockaert, J., and Grau, Y. (1996) Cloning and functional expression of a Drosophila metabotropic glutamate receptor expressed in the embryonic CNS. *J Neurosci* **16**, 6687-6694
13. Krenz, W. D., Nguyen, D., Perez-Acevedo, N. L., and Selverston, A. I. (2000) Group I, II, and III mGluR compounds affect rhythm generation in the gastric circuit of the crustacean stomatogastric ganglion. *J Neurophysiol* **83**, 1188-1201
14. Kucharski, R., Mitri, C., Grau, Y., and Maleszka, R. (2007) Characterization of a metabotropic glutamate receptor in the honeybee (Apis mellifera): implications for memory formation. *Invert Neurosci* **7**, 99-108
15. Washio, H. (2002) Glutamate receptors on the somata of dorsal unpaired median neurons in cockroach, Periplaneta americana, thoracic ganglia. *Zoolog Sci* **19**, 153-162
16. Weinshenker, D., Garriga, G., and Thomas, J. H. (1995) Genetic and pharmacological analysis of neurotransmitters controlling egg laying in C. elegans. *J Neurosci* **15**, 6975-6985
17. Wakabayashi, T., Kitagawa, I., and Shingai, R. (2004) Neurons regulating the duration of forward locomotion in Caenorhabditis elegans. *Neurosci Res* **50**, 103-111
18. Jorgensen, E. M. (2004) Dopamine: should I stay or should I go now? *Nat Neurosci* **7**, 1019-1021
19. Sawin, E. R., Ranganathan, R., and Horvitz, H. R. (2000) C. elegans locomotory rate is modulated by the environment through a dopaminergic pathway and by experience through a serotonergic pathway. *Neuron* **26**, 619-631
20. You, Y. J., Kim, J., Cobb, M., and Avery, L. (2006) Starvation activates MAP kinase through the muscarinic acetylcholine pathway in Caenorhabditis elegans pharynx. *Cell Metab* **3**, 237-245
21. Chalasani, S. H., Chronis, N., Tsunozaki, M., Gray, J. M., Ramot, D., Goodman, M. B., and Bargmann, C. I. (2007) Dissecting a circuit for olfactory behaviour in Caenorhabditis elegans. *Nature* **450**, 63-70
22. Walker, D. S., Gower, N. J., Ly, S., Bradley, G. L., and Baylis, H. A. (2002) Regulated disruption of inositol 1,4,5-trisphosphate signaling in Caenorhabditis elegans reveals new functions in feeding and embryogenesis. *Mol Biol Cell* **13**, 1329-1337
23. Brenner, S. (1974) The genetics of Caenorhabditis elegans. *Genetics* **77**, 71-94
24. Flicek, P., Amode, M. R., Barrell, D., Beal, K., Brent, S., Chen, Y., Clapham, P., Coates, G., Fairley, S., Fitzgerald, S., Gordon, L., Hendrix, M., Hourlier, T., Johnson, N., Kahari, A., Keefe, D., Keenan, S., Kinsella, R., Kokocinski, F., Kulesha, E., Larsson, P., Longden, I., McLaren, W., Overduin, B., Pritchard, B., Riat, H. S., Rios, D., Ritchie, G. R., Ruffier, M., Schuster, M., Sobral, D., Spudich, G., Tang, Y. A., Trevanion, S., Vandrovcova, J., Vilella, A. J., White, S., Wilder, S. P., Zadissa, A., Zamora, J., Aken, B. L., Birney, E., Cunningham, F., Dunham, I., Durbin, R., Fernandez-Suarez, X. M., Herrero, J., Hubbard, T. J., Parker, A., Proctor, G., Vogel, J., and Searle, S. M. (2011) Ensembl 2011. *Nucleic Acids Res* **39**, D800-806
25. Harris, T. W., Antoshechkin, I., Bieri, T., Blasiar, D., Chan, J., Chen, W. J., De La Cruz, N., Davis, P., Duesbury, M., Fang, R., Fernandes, J., Han, M., Kishore, R., Lee, R., Muller, H. M., Nakamura, C., Ozersky, P., Petcherski, A., Rangarajan, A., Rogers, A., Schindelman, G., Schwarz, E. M., Tuli, M. A., Van Auken, K., Wang, D., Wang, X., Williams, G., Yook, K., Durbin, R., Stein, L. D., Spieth, J., and Sternberg, P. W.

(2010) WormBase: a comprehensive resource for nematode research. *Nucleic Acids Res* **38**, D463-467
26. Altschul, S. F., Madden, T. L., Schaffer, A. A., Zhang, J., Zhang, Z., Miller, W., and Lipman, D. J. (1997) Gapped BLAST and PSI-BLAST: a new generation of protein database search programs. *Nucleic Acids Res* **25**, 3389-3402
27. Edwards, R. J., Moran, N., Devocelle, M., Kiernan, A., Meade, G., Signac, W., Foy, M., Park, S. D., Dunne, E., Kenny, D., and Shields, D. C. (2007) Bioinformatic discovery of novel bioactive peptides. *Nat Chem Biol* **3**, 108-112
28. Katoh, K., and Toh, H. (2008) Recent developments in the MAFFT multiple sequence alignment program. *Brief Bioinform* **9**, 286-298
29. Price, M. N., Dehal, P. S., and Arkin, A. P. (2009) FastTree: computing large minimum evolution trees with profiles instead of a distance matrix. *Mol Biol Evol* **26**, 1641-1650
30. Mello, C., and Fire, A. (1995) DNA transformation. *Methods Cell Biol* **48**, 451-482
31. Franks, C. J., Murray, C., Ogden, D., O'Connor, V., and Holden-Dye, L. (2009) A comparison of electrically evoked and channel rhodopsin-evoked postsynaptic potentials in the pharyngeal system of Caenorhabditis elegans. *Invert Neurosci* **9**, 43-56
32. Dillon, J., Hopper, N. A., Holden-Dye, L., and O'Connor, V. (2006) Molecular characterization of the metabotropic glutamate receptor family in Caenorhabditis elegans. *Biochem Soc Trans* **34**, 942-948
33. Tharmalingam, S., Burns, A. R., Roy, P. J., and Hampson, D. R. (2012) Orthosteric and allosteric drug binding sites in the Caenorhabditis elegans mgl-2 metabotropic glutamate receptor. *Neuropharmacology* **63**, 667-674
34. Mitri, C., Parmentier, M. L., Pin, J. P., Bockaert, J., and Grau, Y. (2004) Divergent evolution in metabotropic glutamate receptors. A new receptor activated by an endogenous ligand different from glutamate in insects. *J Biol Chem* **279**, 9313-9320
35. Conn, P. J., and Pin, J. P. (1997) Pharmacology and functions of metabotropic glutamate receptors. *Annu Rev Pharmacol Toxicol* **37**, 205-237
36. Avery, L., and Horvitz, H. R. (1989) Pharyngeal pumping continues after laser killing of the pharyngeal nervous system of C. elegans. *Neuron* **3**, 473-485
37. Rogers, C. M., Franks, C. J., Walker, R. J., Burke, J. F., and Holden-Dye, L. (2001) Regulation of the pharynx of Caenorhabditis elegans by 5-HT, octopamine, and FMRFamide-like neuropeptides. *J Neurobiol* **49**, 235-244
38. Avery, L., and Horvitz, H. R. (1990) Effects of starvation and neuroactive drugs on feeding in Caenorhabditis elegans. *J Exp Zool* **253**, 263-270
39. Enz, R. (2007) The trick of the tail: protein-protein interactions of metabotropic glutamate receptors. *Bioessays* **29**, 60-73
40. Lee, R. Y., Sawin, E. R., Chalfie, M., Horvitz, H. R., and Avery, L. (1999) EAT-4, a homolog of a mammalian sodium-dependent inorganic phosphate cotransporter, is necessary for glutamatergic neurotransmission in caenorhabditis elegans. *J Neurosci* **19**, 159-167
41. Nathoo, A. N., Moeller, R. A., Westlund, B. A., and Hart, A. C. (2001) Identification of neuropeptide-like protein gene families in Caenorhabditiselegans and other species. *Proc Natl Acad Sci U S A* **98**, 14000-14005
42. Kang, C., and Avery, L. (2009) Systemic regulation of starvation response in Caenorhabditis elegans. *Genes Dev* **23**, 12-17
43. Greer, E. R., Perez, C. L., Van Gilst, M. R., Lee, B. H., and Ashrafi, K. (2008) Neural and molecular dissection of a C. elegans sensory circuit that regulates fat and feeding. *Cell Metab* **8**, 118-131

44. Zheng, N., and Raman, I. M. (2011) Prolonged postinhibitory rebound firing in the cerebellar nuclei mediated by group I metabotropic glutamate receptor potentiation of L-type calcium currents. *J Neurosci* **31**, 10283-10292
45. Avery, L., and You, Y. J. (2012) C. elegans feeding. *WormBook*, 1-23

Acknowledgements: JCD was supported by a Biotechnology and Biological Sciences Research Council (BBSRC) committee studentship; grant number BB/F009208/1 and the Gerald Kerkut Charitable Trust. CF and CM were supported by the BBSRC. FC was supported by a grant-fellowship number EF0002 from Consejería de Salud, Junta de Andalucía, Spain. Some strains were provided by the Caenorhabditis Genetics Centre (CGC), which is funded by National Institutes of Health Office of Research Infrastructure Programs (P40 OD010440)

FOOTNOTES

[1]Franks, CJ., Murray, C., Ogden, D., O'Connor, V., Holden-Dye, L. (2010) Investigating the Role of UNC-31 in Glutamatergic Signaling in the Pharynx. *Meeting Abstract, European C. elegans Neurobiology Meeting,Crete.*

[2]Dalliere, N., Bhatla, N., Walker, R., O'Connor, V., Holden-Dye, L. (2014) Pumping off Food (PoffF) reveals a glutamate dependent microcircuit that imposes cue dependent inhibitory tone on the pharynx. *Meeting Abstract, Neuronal Development, Synaptic Function and Behaviour, Madison, WI.*

[3]Ishihara, T and Katsura I. (1996) Metabotropic glutamate receptor in *C. elegans*. *Worm Breeder's Gazette,* 14(3), 40.

FIGURE LEGENDS

Figure 1. Molecular characterisation of the different *mgl* receptor subtypes. Exon-intron boundaries characterised by the analysis of SL-1 PCR amplified and RACE amplified cDNA fragments are shown for each *mgl* subtype. For comparison the gene models annotated by Wormbase version WS243 are shown. (▼) SL-1 trans-splice site (▽) alternative splice donor site leading to a 6 nucleotide insertion. The position of the putative *maf-1* ATG start codon is indicated in the diagram of the *mgl-2* gene models. White boxes represent 5' and 3' untranslated regions. Scale bars: 500bp

Figure 2. Unrooted molecular phylogeny of the mGluR family with subfamily clades represented by single branches for clarity. The root position using vertebrate taste receptors as an outgroup (not shown) is indicated with a filled arrow. The position given by midpoint rooting of the mGluR family alone is indicated with an open arrow. Bootstrap values for the main MGR groups are shown (1000 replicates). Vertebrate mGluR GRM1-8, nematode MGL1-3 and *Drosophila* mGluRA and mGluRB are labelled. Other sequences are indicated with taxa only.

Figure 3. The *mgl* subtypes have distinct and overlapping expression patterns in the *C. elegans* nervous system. The expression of *mgl-1::GFP* is widespread, in neurons located in **A.** The nerve ring and **B.** the tail**.** De-sheathing the pharynx by removing the overlaying cuticle and muscle identified *mgl-1::GFP* expression in neurons of the pharyngeal nervous system **C**. *mgl-2::GFP* fluorescence was recorded in **D.** the nerve ring, **E** the tail and **F** the pharyngeal nervous system. *mgl-3::GFP* fluorescence was observed in **G.** the nerve ring and the pharyngeal nervous system and **H.** the tail. The white dotted lines indicate the outer perimeter of the preparation of the whole worm (**A, B, D, E, G, H**) and the unsheathed pharyngeal preparation (**C, F**). Each of the *mgl* subtypes is expressed in the pharyngeal NSM neurons, indicated by the white arrow heads.

Figure 4. Selective mGluR agonists trans-ACPD and LCCG-I both inhibit the activity of the pharyngeal neuromuscular network. A. EPG recording configuration from the semi-intact pharyngeal preparation.Trace **B.** and **C**. each show an EPG recorded from individual pharynxes of wild-type worms. Each deflection represents a single pharyngeal pump (because of the long time-base individual pumps cannot always be resolved if the pumping activity is fast). The period of drug application is indicated on individual recordings. **D.** Concentration-response curve for the effect of LCCG-I on the percentage change in the rate of pharyngeal pumping recorded in the EPG configuration. Each point is the mean ± s.e.m of n = 9 determinations. **E.** Intracellular recording configuration to measure pharyngeal muscle activity. **F.** The effect of 10μM LCCG-I on the frequency of pharyngeal action potentials recorded intracellularly from the *C. elegans* pharyngeal terminal bulb muscle. The period of drug application is indicated on the recording by the solid black line, with the concentration indicated beneath.

Figure 5. The effects of LCCG-I on the EPG recorded from the pharyngeal muscle of *mgl* receptor subtype mutants. A-C, EPG's recorded from individual *mgl* mutant pharynxes. The point of LCCG-I drug application is indicated on individual recordings by solid lines, with the concentration indicated beneath. **D.** Concentration-response of *mgl-1(tm1811)* and the genomic rescue *mgl-1(tm1811);ZC506* (the wild-type response is included for comparison). For *mgl-1(tm1811)* each point is the mean ± s.e.m of n = 12 determinations. For *mgl-1(tm1811)* genomic rescue 10 individual pharynxes were tested (5 from each of two stable transgenic lines transformed with ZC506). Each point is the mean ± s.e.m of n = 10 determinations. **E.** Concentration-response for the effects of LCCG-I on *mgl-2(tm0355)* and *mgl-3(tm1766)*. Each point is the mean ± s.e.m of n = 6 determinations for *mgl-2(tm0355)* and n = 5 for *mgl-3(tm1766)*.

Figure 6. A comparison of excitatory pharyngeal muscle responses in the desheathed pharyngeal preparation of wild-type (N2) and glutamate deficient (*eat-4*) worms following optogenetic activation of glutamatergic pharyngeal neurons. A. A representative trace to show that a 1 msec pulse of blue light (470nm) did not excite the pharynx of N2 worms that do not express *Peat-4::ChR2;mRFP*. The stimulus is indicated in the trace below the voltage response recorded from the muscle. **B.** Representative traces of the light stimulated postsynaptic potentials recorded from the pharyngeal muscle of N2 and *eat-4(ky5)* worms expressing *Peat-4::ChR2;mRFP*. Note that the postsynaptic response still occurs in *eat- 4(ky5)* but the latency is longer. **C.** The latency of the light activated PSP is significantly longer in *eat-4(ky-5)* compared to N2. *eat-4(ky5);[Peat-4::ChR2;mRFP]* (n = 8) and *N2;[Peat-4::ChR2;mRFP]* (n = 14). Results are presented as the mean ± s.e.m. **p<0.01 in an unpaired Student's t-test.

Figure 7. The effect of LCCG-I on light evoked post-synaptic potentials in the desheathed pharyngeal preparation of wild-type and *mgl-1(tm1811)* worms. A. Representative light evoked post-synaptic responses in N2 wild-type worms expressing *Peat-4::ChR2;mRFP* before, during and after the application of 10μM LCCG-I. The stimulus is indicated in the trace below the voltage response recorded from the muscle. Quantification of the LCCG-I inhibition of full action potentials evoked by light activation of *Peat-4::ChR2* in **B.** wild-type *(n* = 10) and **C.** *mgl-1(tm1811) (n* = 7) worms. A post-synaptic potential was considered to be light-evoked if it occurred within 50msec of the stimuli, otherwise it was considered as arising from the spontaneous intrinsic activity of the pharynx and not included in the analysis.

Figure 8. The effect of acute and longer term food deprivation upon the regulation of pharyngeal pumping in *mgl* mutant animals. A. A diagram indicating the time line of the pharyngeal pumping assay. **B.** The rate of pumping on and off food at the time points indicated in Figure A for N2 (n = 39), *mgl-1(tm1811)* (n = 27), *mgl-2(tm0355)* (n = 28), *mgl-3(tm1766)* (n = 17) and *mgl-1(tm1811);mgl-3(tm1766)* (n = 30). Significance was determined using the one-way ANOVA and Bonferroni post-test comparisons to compare *mgl* mutant pumping to wild-type pumping.

*p<0.05 in Bonferroni post-test comparisons. **C.** The rate of pumping 5 minutes after removal from food to assess rescue against the *mgl-1* exaggerated OFF-food phenotype by the cosmid ZC506. N2 (*n* = 15), *mgl-1(tm1811)* (*n* = 15) and the rescue *mgl-1(tm1811);ZC506* (*n* = 15). Significance was determined using an unpaired Student's t-test to compare *mgl-1(tm1811)* and *mgl-1(tm1811);ZC506* to wild-type pumping.

FIGURE 1

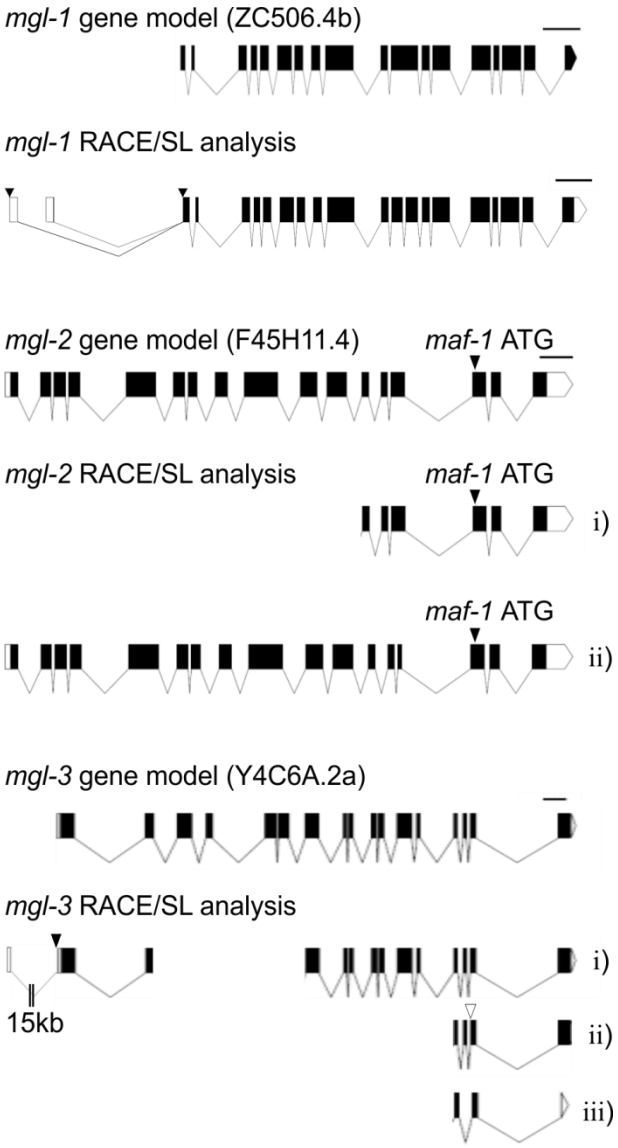
mgl-1 gene model (ZC506.4b)
mgl-1 RACE/SL analysis
mgl-2 gene model (F45H11.4)
maf-1 ATG
mgl-2 RACE/SL analysis
maf-1 ATG
i)
maf-1 ATG
ii)
mgl-3 gene model (Y4C6A.2a)
mgl-3 RACE/SL analysis
i)
15kb
ii)
iii)

FIGURE 2

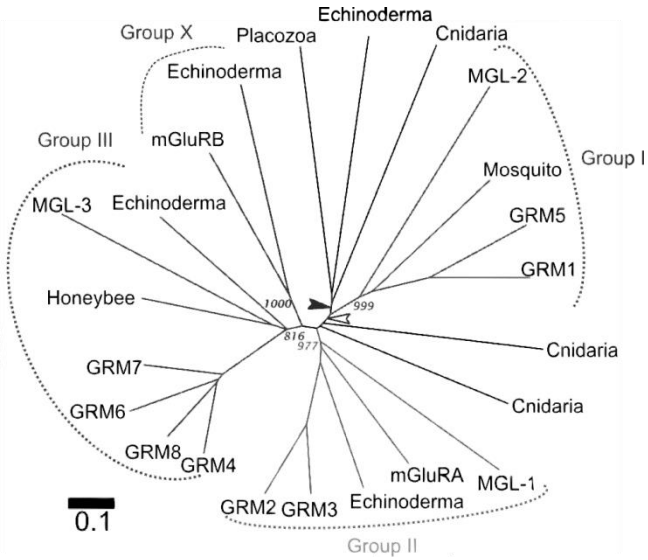
Group X
Placozoa
Echinoderma
Cnidaria
Echinoderma
MGL-2
Group III
mGluRB
Group I
Mosquito
MGL-3
Echinoderma
GRM5
GRM1
Honeybee
1000
999
816
977
Cnidaria
GRM7
Cnidaria
GRM6
GRM8
GRM4
mGluRA
MGL-1
0.1
GRM2
GRM3
Echinoderma
Group II

FIGURE 3

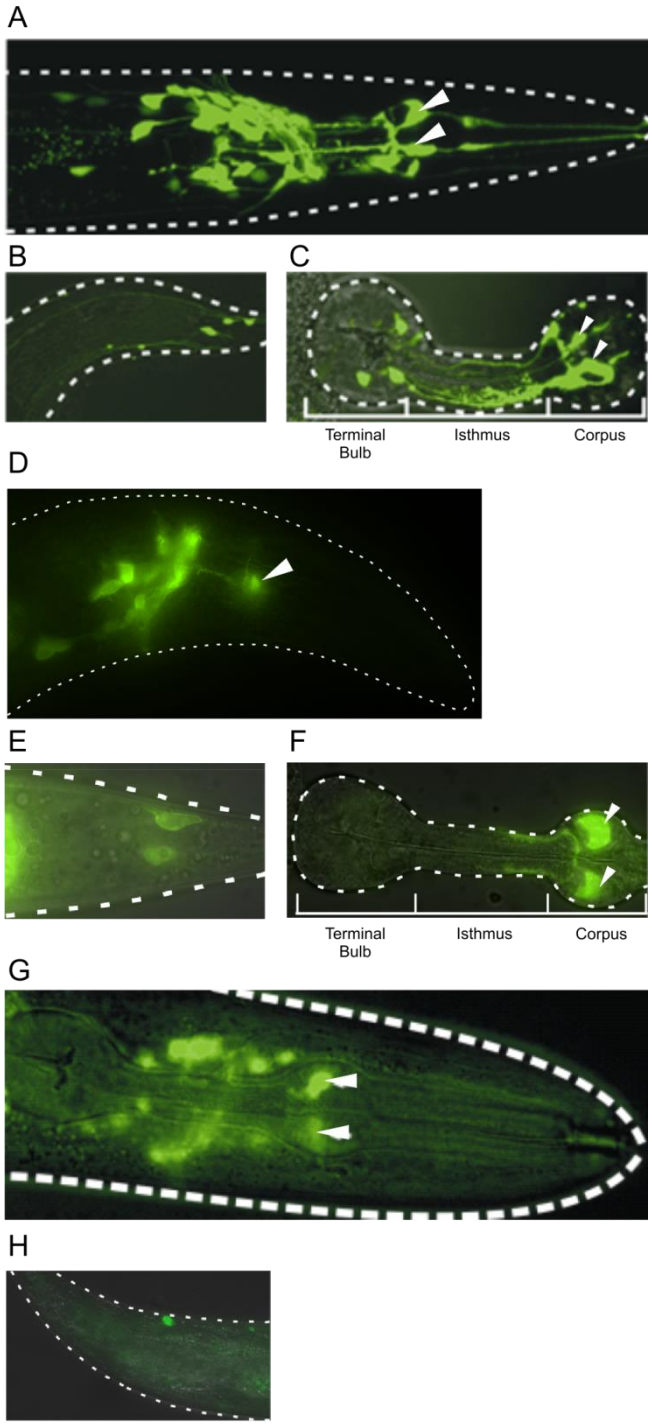
A
B
C
Terminal Bulb
Isthmus
Corpus
D
E
F
Terminal Bulb
Isthmus
Corpus
G
H

FIGURE 4

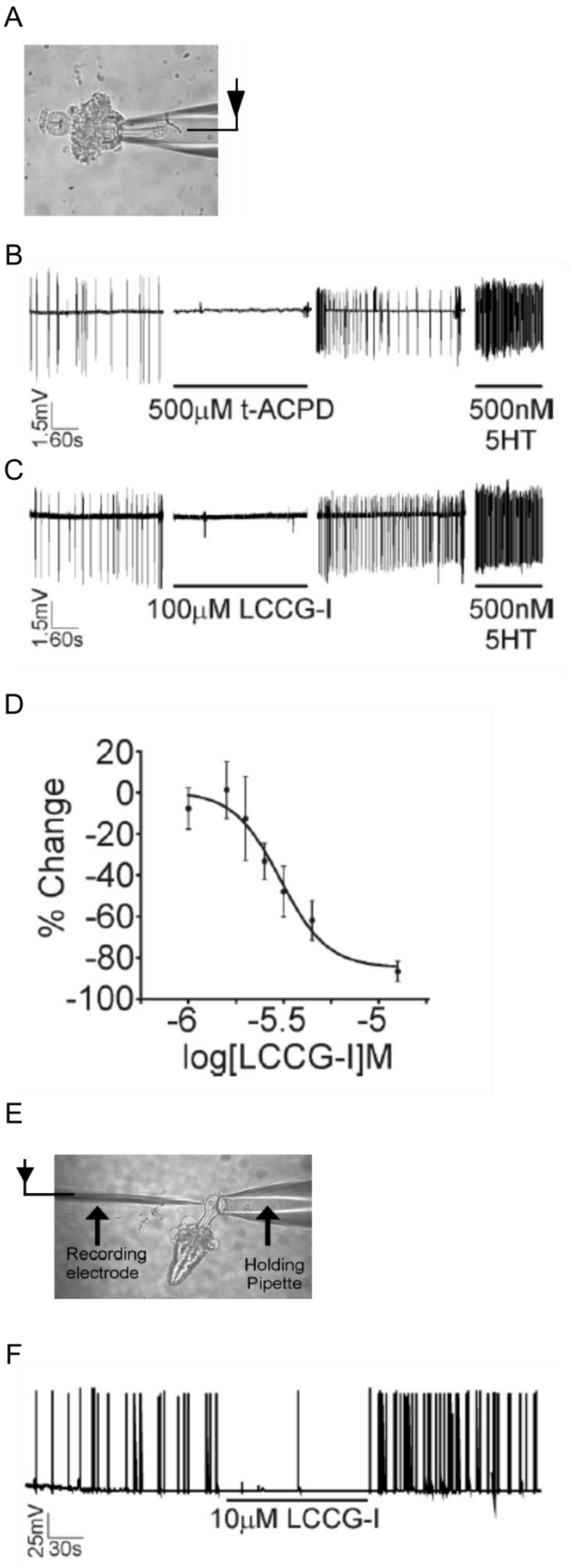
A
B
1.5mV
60s
500μM t-ACPD
500nM
5HT
C
1.5mV
60s
100μM LCCG-I
500nM
5HT
D
% Change
20
0
-20
-40
-60
-80
-100
-6
-5.5
-5
log[LCCG-I]M
E
Recording
electrode
Holding
Pipette
F
25mV
30s
10μM LCCG-I

FIGURE 5

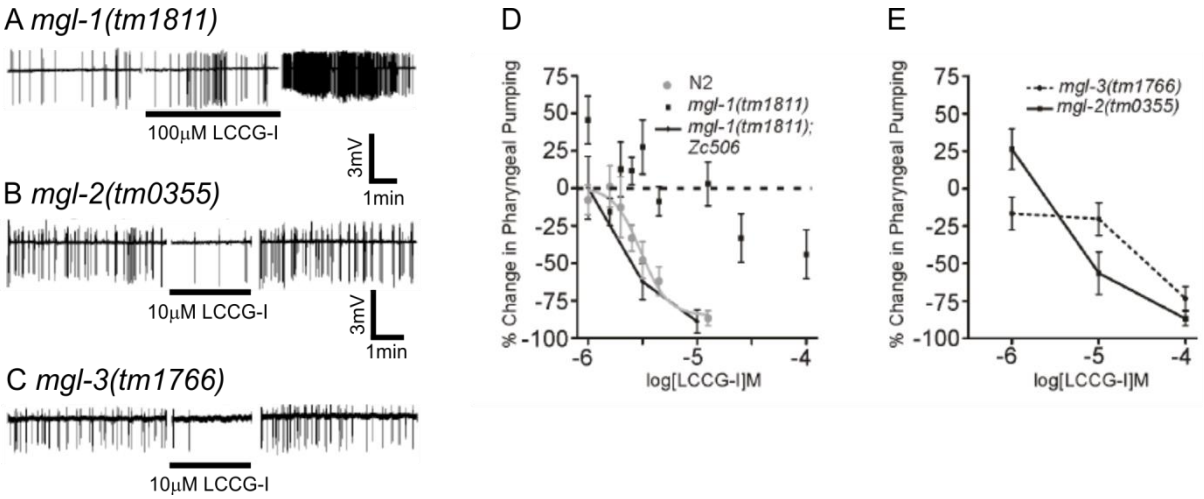
A mgl-1(tm1811)
100μM LCCG-I
3mV
1min
B mgl-2(tm0355)
10μM LCCG-I
3mV
1min
C mgl-3(tm1766)
10μM LCCG-I
D
% Change in Pharyngeal Pumping
N2
mgl-1(tm1811)
mgl-1(tm1811); Zc506
log[LCCG-I]M
E
% Change in Pharyngeal Pumping
mgl-3(tm1766)
mgl-2(tm0355)
log[LCCG-I]M

FIGURE 6

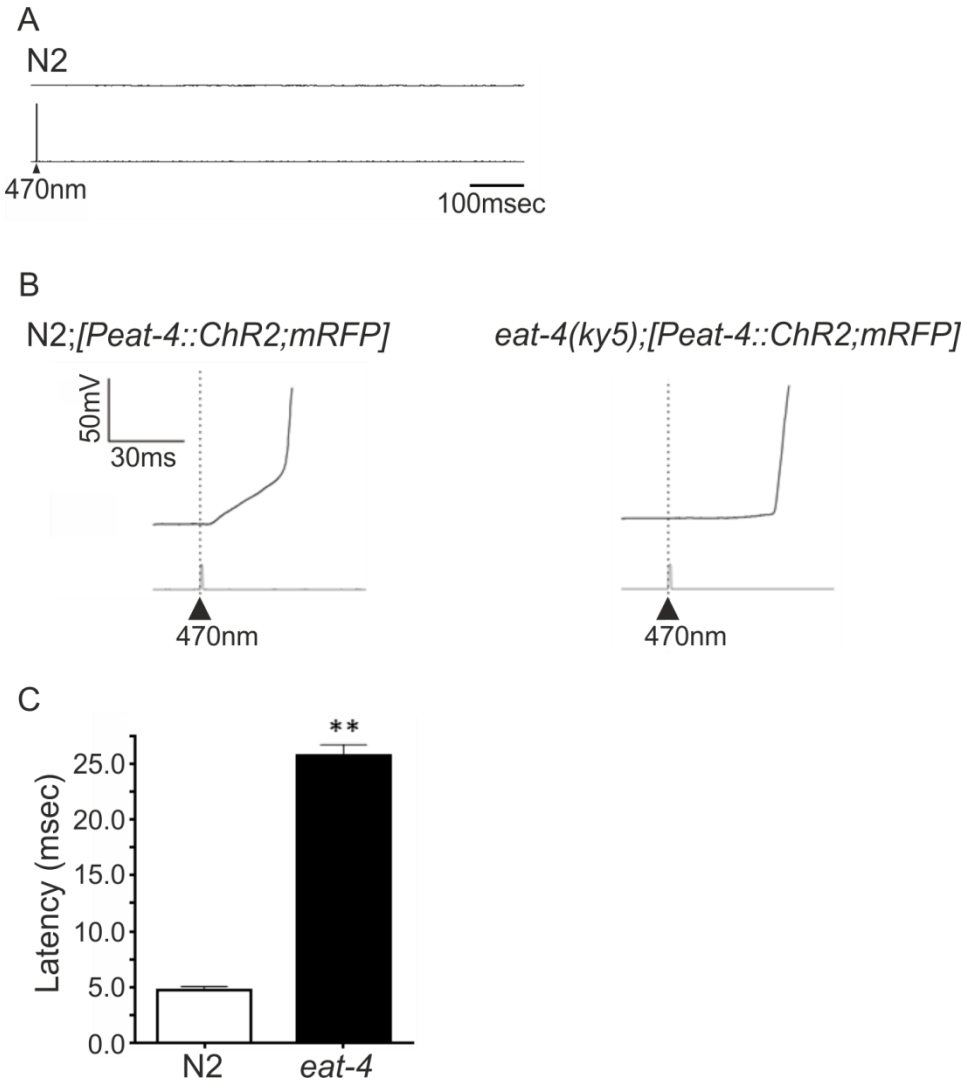
A
N2
470nm
100msec
B
N2;[Peat-4::ChR2;mRFP]
eat-4(ky5);[Peat-4::ChR2;mRFP]
50mV
30ms
470nm
470nm
C
Latency (msec)
25.0
20.0
15.0
10.0
5.0
0.0
**
N2
eat-4

FIGURE 7

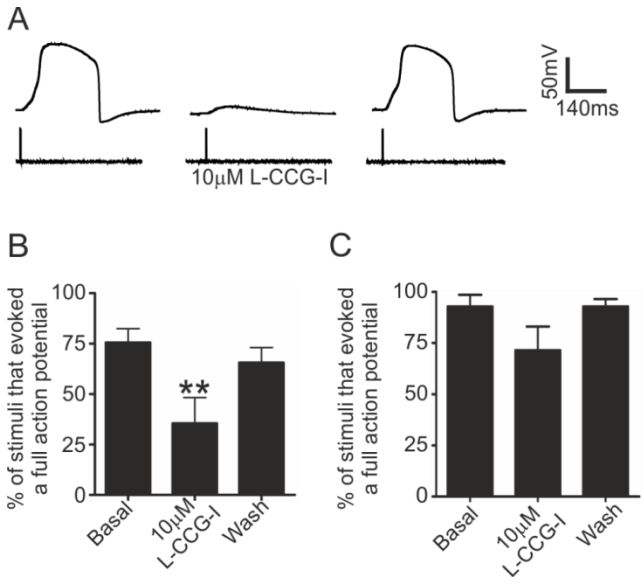
A
50mV
140ms
10μM L-CCG-I
B
% of stimuli that evoked a full action potential
100
75
50
25
0
**
Basal
10μM L-CCG-I
Wash
C
% of stimuli that evoked a full action potential
100
75
50
25
0
Basal
10μM L-CCG-I
Wash

FIGURE 8

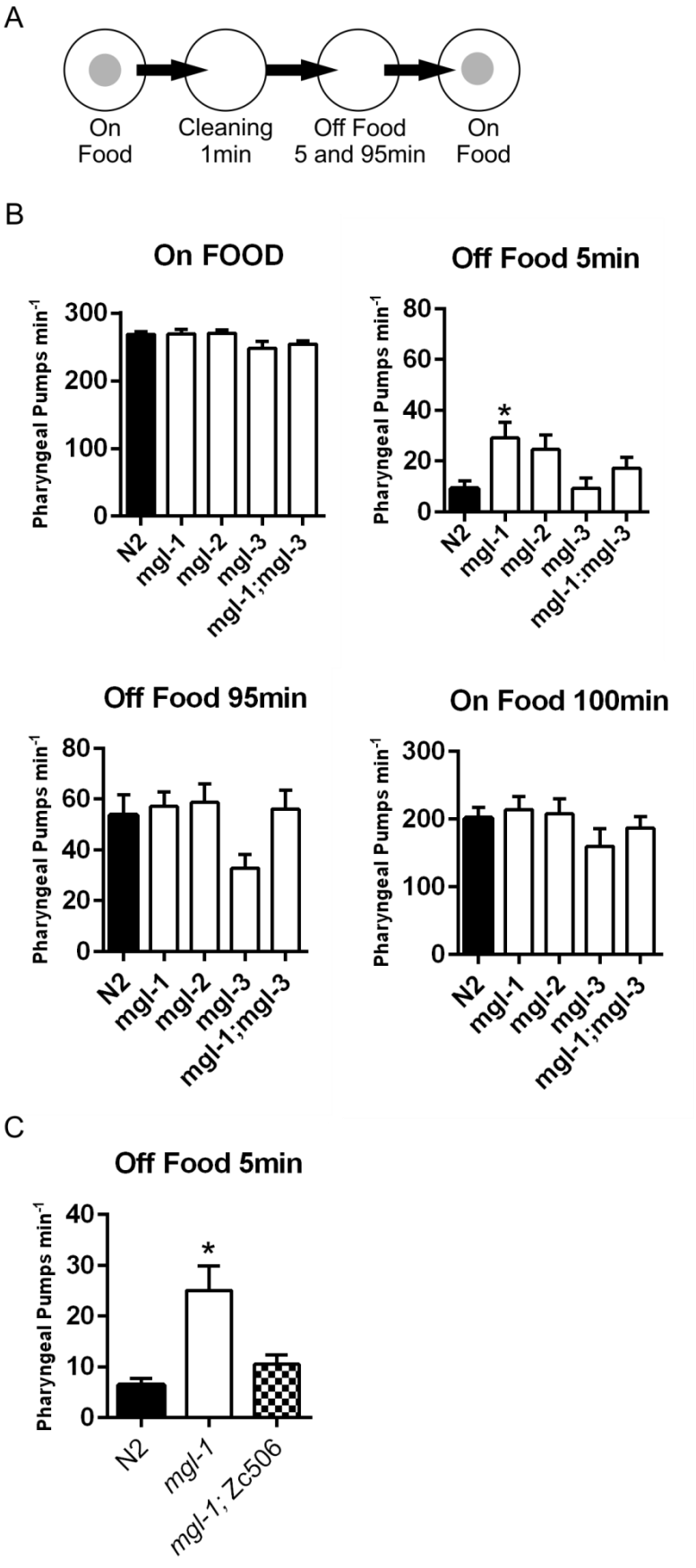
A
On Food
Cleaning 1min
Off Food 5 and 95min
On Food
B
On FOOD
Off Food 5min
Off Food 95min
On Food 100min
Pharyngeal Pumps min-1
N2
mgl-1
mgl-2
mgl-3
mgl-1;mgl-3
C
Off Food 5min
mgl-1; Zc506